Validation of runaway electron models using synchrotron radiation measurements and full-orbit simulations

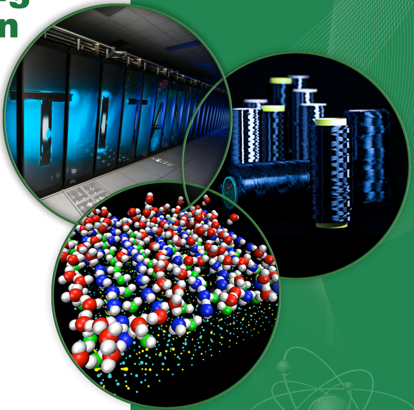

D. del-Castillo-Negrete[1]
L. Carbajal[1]
C. Paz-Soldan[2]

[1]Oak Ridge National Laboratory
[2]General Atomics, San Diego CA

Theory and Simulation of Disruptions Workshop

PPPL
Princeton, NJ
July 16-18, 2018

ORNL is managed by UT-Battelle
for the US Department of Energy

OAK RIDGE National Laboratory

SYNCHROTRON RADIATION ROUTINELY MEASURED TO INFER RE INFORMATION

Very valuable diagnostic to validate RE models

This motivates the need of accurate synthetic diagnostics

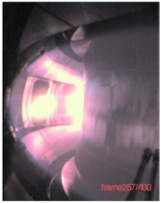

Visible camera in EAST [Y. Shi et al. Rev. Sci. Instrum. **81,** 033506 (2010)].

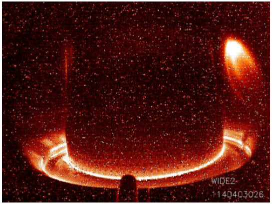

Visible camera in C-Mod [A. Tinguely et al. APS DPP 2016].

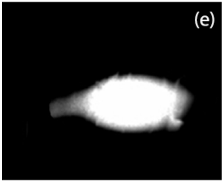

IR camera in TEXTOR [K. Wongrach et al. Nucl. Fusion **54,** 043011 (2014)].

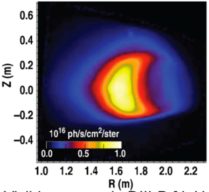

Visible camera in DIII-D [J. H. Yu et al. PoP **20**, 042113 (2013)].

KORC (Kinetic Orbit Runaway electrons Code)

- State of the art, unique, recently develop code to study **full orbit space-dependent** effects
- Relativistic dynamics of runaway electrons span a huge range of scales 10^{-11} sec to 10^{-3}-1 sec
- **KORC uses two levels of description:**
  - **KORC-GC** averages the fast gyro-motion allowing to compute long-term dynamics.
  - **KORC-FO** integrates the exact dynamics resolving all the scales allowing to compute short-term detailed orbit-dependent physics in 6-D phase space.
- Both versions include Monte-Carlo collision operators with background plasma and impurities as well as synchrotron radiation reaction forces.
- KORC can be run with analytical or numerically generated electromagnetic fields, e.g. VMEC, SIESTA, EFIT, JFIT and NIMROD.
- Recent developments include a synchrotron radiation synthetic diagnostic.

Orbits in ITER computed with **KOC-GC**
Using VMEC magnetic field

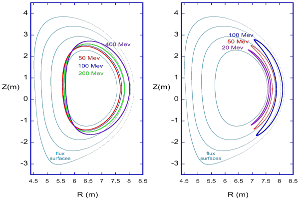

Orbits in DIII-D computed with **KORC-FO**
using JFIT magnetic field

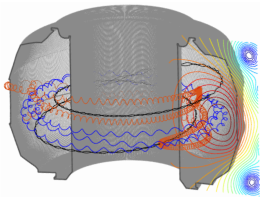

KORC SYNCHROTRON EMISSION SYNTHETIC DIAGNOSTIC

Computes $P(\lambda, \psi, \chi)$ using the full-orbit information of large ensembles of RE incorporating the basic camera geometry

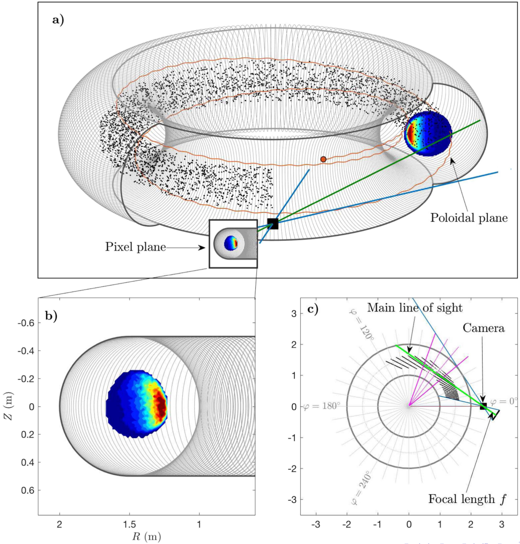

SYNCHROTRON RADIATION: PASSING PARTICLES

- The total radiation power $P_T = \frac{e^2}{6\pi\epsilon_0 c^3}\gamma^4 v^4 \kappa^2$ depends on the geometry of the orbit through the curvature

$$\kappa = \frac{e}{\gamma m_e v^3}\left|\mathbf{v} \times (\mathbf{v} \times \mathbf{B})\right| = \frac{eB}{\gamma m_e v}\sin\theta$$

  where B and θ are functions of the particle potion $\mathbf{r} = \mathbf{r}(t)$.
- Approximating κ assuming θ and/or B constant (as done in reduced models) can introduce significant errors in P_T

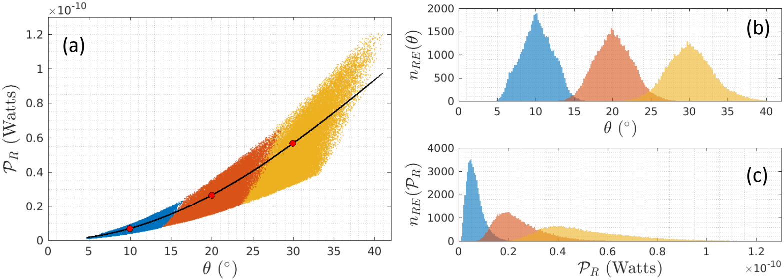

Passing $\mathcal{E} = 30\,\mathrm{MeV}$ particles in axisymmetric field.

SYNCHROTRON RADIATION: TRAPPED PARTICLES

Scatter plots in the $(\theta, \mathcal{P}_R)$ plane and histograms of number of runaways with a given pitch angle and a given radiated power.

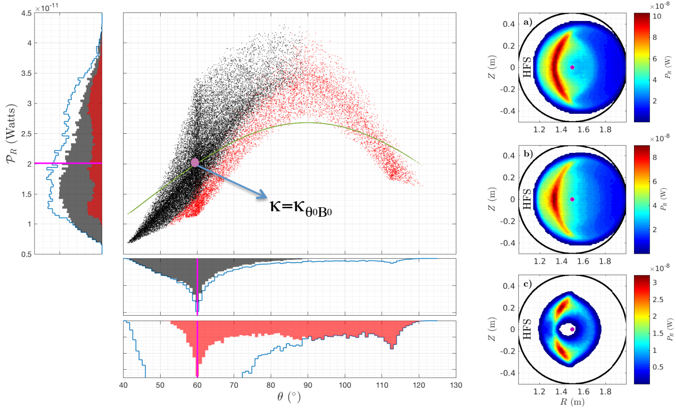

Plots on the right: radiation in poloidal plane for the total, (a), passing only, (b), and trapped only, (c), runaway electrons.
Axisymmetric magnetic field, $\mathcal{E}_0 = 10$ MeV and $\theta_0 = 60^o$

RUNAWAY ELECTRONS IN THE PRESENCE OF MAGNETIC ISLANDS AND STOCHASTICITY

(a) Poincare plot of NIMROD diverted DIII-D magnetic field.
(b) Spatial distribution of runaway electrons

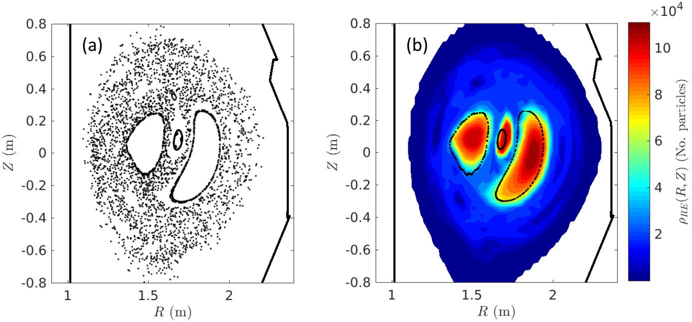

$\mathcal{E}_0 = 13$ MeV, mono-pitch, $\theta_0 = 8.6^{\rm o}$.

SYNCHROTRON RADIATION IN THE PRESENCE OF MAGNETIC ISLANDS AND STOCHASTICITY

3-D magnetic field effects on synchrotron spectra

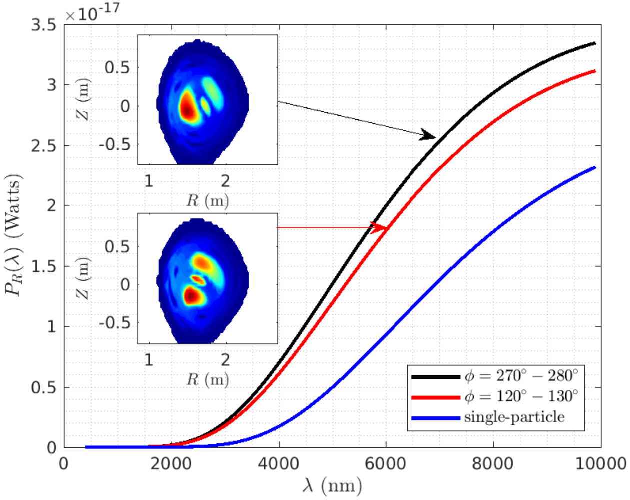

$\mathcal{E}_0 = 13$ MeV $\theta_0 = 8.6^{\text{o}}$ NIMROD diverted DIII-D magnetic field

MODEL VALIDATION USING SYNCHROTRON RADIATION MEASUREMENTS

- Our goal is to use KORC simulations and recent DIII-D synchrotron radiation measurements to validate RE models.
- The experimental results correspond to DIII-D quiescent plasma shot # 165826 reported in [Paz-Soldan, et al. Phys. of Plasmas **25** 056105 (2018); Phys. Rev. Lett. **118** 255002 (2017)]. Visible camera image:

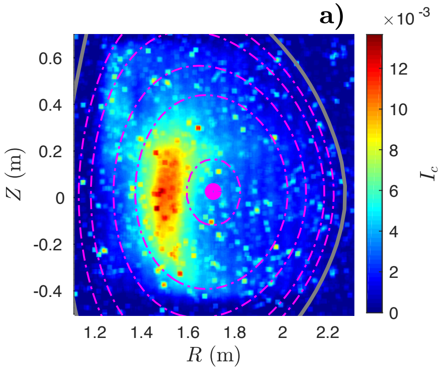

RECENT MODELING STUDIES USING SOFT+CODE [*]

DIII-D measured Radiation pattern

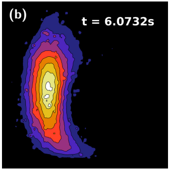

Fig. 3-(b) Ref.[*]

CODE computed distribution functions

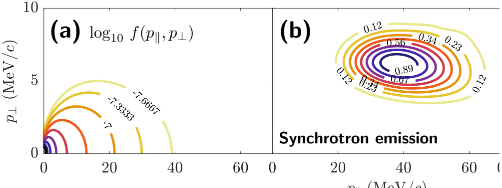

Fig. 5-(a)-(b) Ref.[*]

SOFT+CODE Computed radiation pattern

Radial profiles

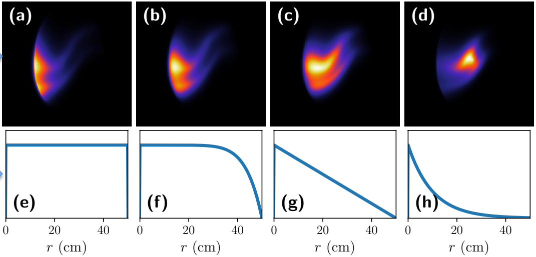

Fig. 6 Ref.[*]

[*] M. Hoppe, O. Embréus, C. Paz-Soldan, R.A. Moyer and T. Fülöp. Nucl. Fusion **58** 082001 (2018).

RE ENERGY DISTRIBUTION FUNCTION

- The energy distribution of the RE is taken directly from the experimental measurements in [Paz-Soldan, et al. Phys. Rev. Lett. **118** 255002 (2017)]

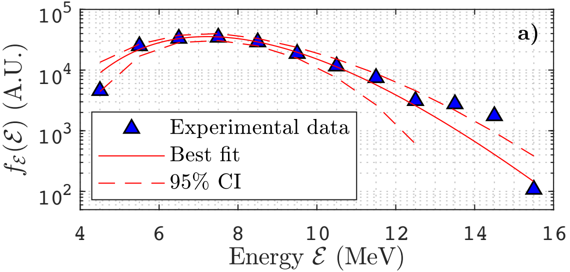

- We sampled the RE energy from a fitted distribution of the form

$$f_{\mathcal{E}}(\mathcal{E}) = \frac{1}{\Gamma(\alpha)\epsilon^{\alpha}} \mathcal{E}^{\alpha-1} \exp\left(-\frac{\mathcal{E}}{\epsilon}\right)$$

with $\alpha = 15.38$ and $\epsilon = 0.50$.

RE PITCH ANGLE DISTRIBUTION FUNCTION

- The pitch angle distributions is not well-resolved in experiments and it is the focus of our model validation efforts.
- We assume a pitch angle distribution of the form

$$f_\theta(\theta, \mathcal{E}) = \frac{A}{2\sinh A}\exp\left(A\cos\theta\right) \,,$$

  where

$$A = \hat{A}\,\mathcal{C}\frac{p^2}{\sqrt{p^2+1}} \,, \qquad \mathcal{C} = \frac{2\bar{E}}{Z_{eff}+1}$$

- The normalized electric field and Z_{eff} is taken from the experiment, $\bar{E} = 4.0$ and $Z_{eff} = 4.5$.
- The value $\hat{A} = 1$ exactly corresponds to the standard Fokker-Planck model based on the equilibration of electric field acceleration and pitch angle scattering.
- **In the validation study we will take $\hat{A}$ as a free parameter and study the dependence of the synchrotron radiation on its value.**

RE SPATIAL DISTRIBUTION FUNCTION

- We will assume an initial spatially homogeneous toroidal distribution of RE with elliptical cross section with radius r_0 matching the flux-surfaces (red curve).
- As expected, the radial drifts shift the distribution to the low field side and spreads the beam boundary.

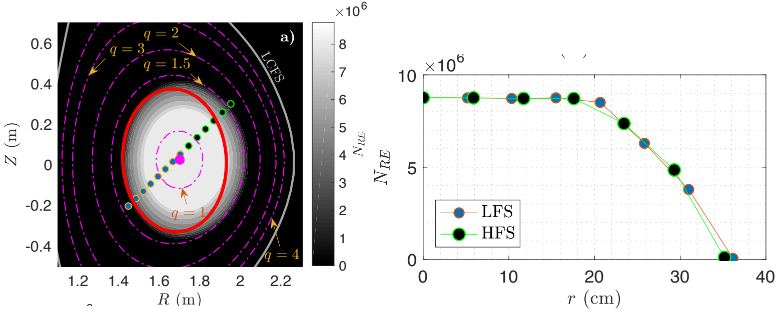

- **In the validation study we will take r_0 as a free parameter and study the dependence of the synchrotron radiation on its value.**

RADIATION POWER DISTRIBUTION FUNCTION

Synchrotron radiation per particle

$$P_R(\theta, \mathcal{E}, \lambda, B_0) = \frac{1}{\sqrt{3}} \frac{ce^2}{\epsilon_0 \lambda^3} \left(\frac{mc^2}{\mathcal{E}} \right)^2 \int_{\lambda_c/\lambda}^{\infty} K_{5/3}(\eta) d\eta$$

Weighted radiation power distribution

$$\mathcal{P}_R = f_{RE}(\theta, \mathcal{E}) \times P_R(\theta, \mathcal{E}, \lambda, B_0)$$

Total radiation power $P_T = \int_0^\infty \int_0^\pi \mathcal{P}_R(\theta, \mathcal{E}, \lambda, B_0) \sin\theta d\theta d\mathcal{E}$

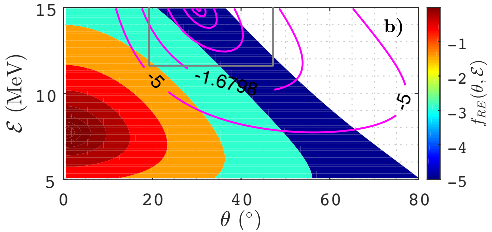

Measured SR comes mainly from RE with large pitch angles and energies, i.e. the tails of the distribution ($B_0 = 1.8$T)

MEASURED SPATIAL DISTRIBUTION OF SYNCHROTRON RADIATION [1]

- DIII-D quiscent plasma shot # 165826
- Visible camera image at $t \approx 5045$ ms.

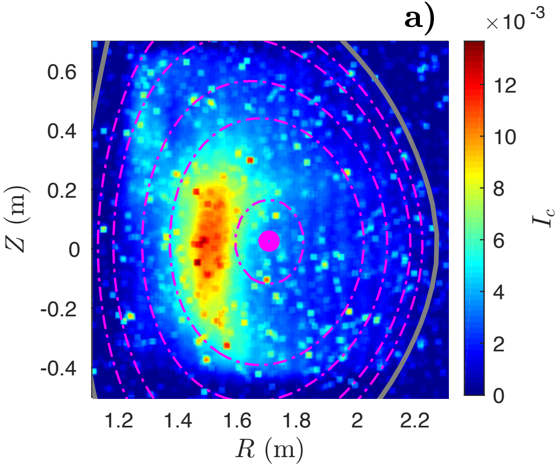

[1] Paz-Soldan, et al. Phys. of Plasmas **25** 056105 (2018).

PROPER ORTHOGONAL DECOMPOSITION
Singular Value Decomposition (SVD)

- Camera image represented as an $NY \times NX$ matrix I_c.
- The SVD decomposition of I_c is given by:

$$I_c = U\,S\,V^T$$

  where U and V are unitary matrices and S is a diagonal matrix with the singular values.
- The columns of U, $\{u^{(k)}\}$, and V, $\{v^{(k)}\}$ form a set of orthonormal vectors and I_c can be written as the weighted, ordered sum of separable matrices $M^{(k)}$

$$I_c = \sum_{k=1}^{\mathfrak{R}} s_k u^{(k)} \otimes v^{(k)} = \sum_{k=1}^{\mathfrak{R}} s_k M^{(k)} \,,$$

  where $\mathfrak{R}$ denotes the rank of I_c, and $\otimes$ is the tensor product.

PROPER ORTHOGONAL DECOMPOSITION

Low rank approximation: denoising and principal components

- For $r < \mathfrak{R}$, the low rank-r approximation of I_c is defined as

$$I_c^{(r)} = \sum_{k=1}^{r} s_k M^{(k)} \approx I_c$$

- The Eckart-Young theorem guarantees that $I_c^{(r)}$ is the best rank-r approximation of I_c in the Frobenius norm

$$E(r) = \sqrt{\sum_{i,j} \left| I_{c\,ij} - I_c^{(r)}{}_{ij} \right|^2}$$

- The low rank-r approximation denoises the image because it eliminates the high order (low energy) modes.
- The low rank-r modes correspond to the principal components, i.e. the modes that capture the main features of the data (in terms of energy content).

PROPER ORTHOGONAL DECOMPOSITION: IMAGE DENOISING

Rank-3 representation of pixel camera data

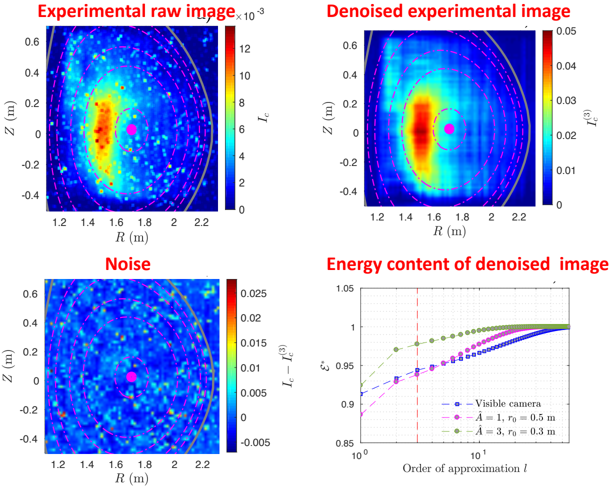

MODEL VALIDATION STRATEGY

- We assume a pitch angle distribution of the form

$$f_\theta(\theta, \mathcal{E}) = \frac{A}{2\sinh A} \exp\left(A\cos\theta\right) , \qquad A = \hat{A}\,\mathcal{C}\frac{p^2}{\sqrt{p^2+1}}$$

  and a spatially homogeneous toroidal distribution with elliptical cross section of size r_0.
- We consider $\hat{A}$ and r_0 as free parameters.
- The rest of the parameters are taken directly from the experiment.
- The value $\hat{A} = 1$ exactly corresponds to the standard Fokker-Planck model based on the equilibration of electric field acceleration and pitch angle scattering.
- The goal is to search for the values of $\hat{A}$ and r_0 for which the synthetic data obtained from KORC matches the experiment.

PROPER ORTHOGONAL DECOMPOSITION: DOMINANT MODES

Rank-1 SVD modes of pixel camera data

$$I_c \approx s_1 u^{(1)}(Z) \otimes v^{(1)}(R)$$

- The use of the rank-1 SVD modes allows the possibility of comparing the experimental and synthetic data using optimal one-dimensional functions along the R and Z directions.

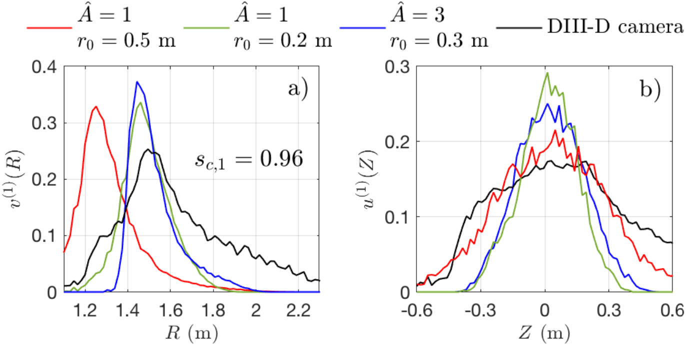

COMPARISON OF MEAN POSITION AND WIDTH OF RADIATION SPOT

$$\overline{R} = \frac{\int R v^{(1)}(R) dR}{\int v^{(1)}(R) dR}, \qquad \Delta R = \frac{2\int (R - \overline{R})^2 v^{(1)}(R) dR}{\int v^{(1)}(R) dR}$$

$$\overline{Z} = \frac{\int Z u^{(1)}(Z) dZ}{\int u^{(1)}(Z) dZ} \qquad \Delta Z = \frac{2\int (Z - \overline{Z})^2 u^{(1)}(Z) dZ}{\int u^{(1)}(Z) dZ}$$

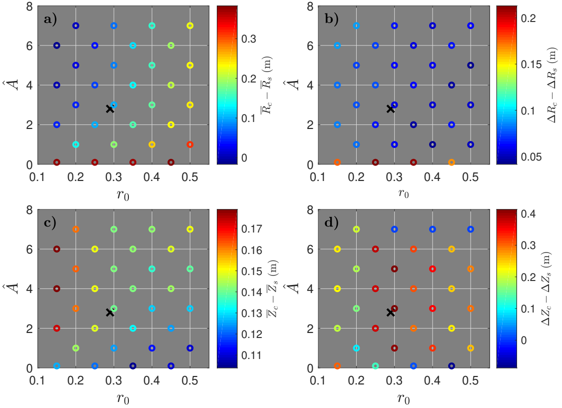

COMPARISON OF SPATIAL DISTRIBUTION OF RADIATION

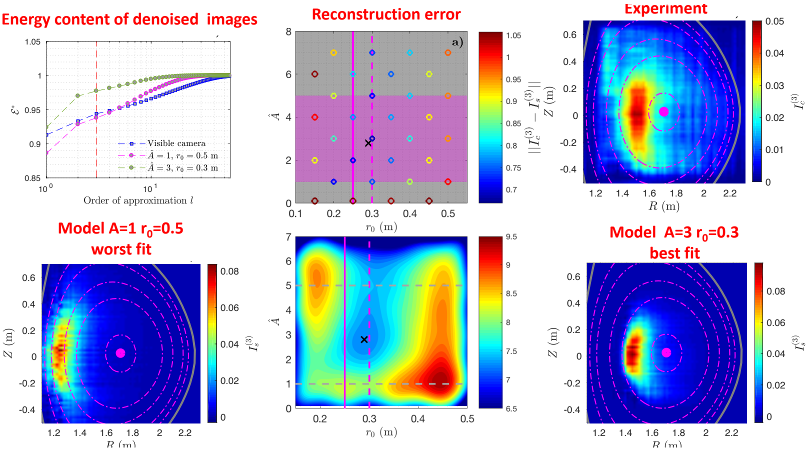

- In the experiment $\hat{A} \sim (1, 5)$, inferred size of RE beam $r_0 \sim 0.25$, inferred size from energy profile $r_0 \sim 0.3$ [Paz-Soldan, et al. Phys. Rev. Lett. **118** 255002 (2017)]

MODEL VALIDATION USING LARGE-TIME PARTICLE SIMULATIONS

- In the previous section we discussed model validation using synchrotron emission data and KORC numerical simulations that tracked RE in relatively short times $\sim 10\mu\,\mathrm{sec}$.
- To complement this study we consider now simulations of large ensembles of RE for times up to $\sim 35\,\mathrm{msec}$.
- The main goal is to validate if the Fokker-Planck pitch angle distribution model remains an equilibrium distribution when spatially-dependent orbit effects are included.
- The simulations include the electric field acceleration, the geometry of the magnetic field using an EFIT magnetic equilibrium, and collisions with the background plasma and impurities incorporating the $n_e(r)$, $T_e(r)$ and $Z_{eff}(r)$ plasma profiles.

PLASMA STATE

The profile information is used in the local (spatial) dependence of the collisional frequencies on $n_e(r)$, $T_e(r)$ and $Z_{eff}(r)$.

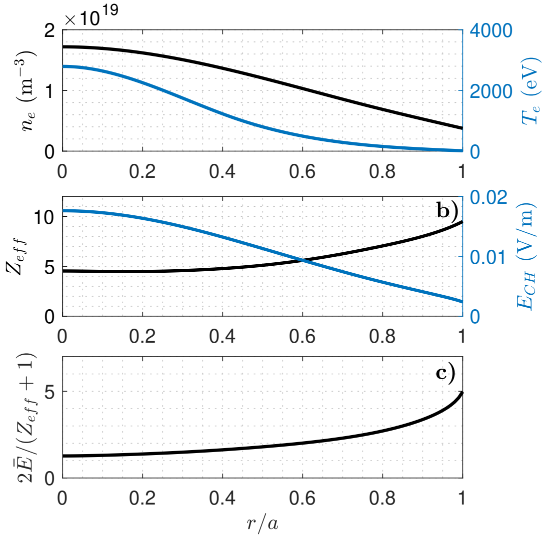

MODEL VALIDATION USING LARGE-TIME SIMULATIONS

- Since, as discussed before, the main contribution to the measured radiation comes from the tails

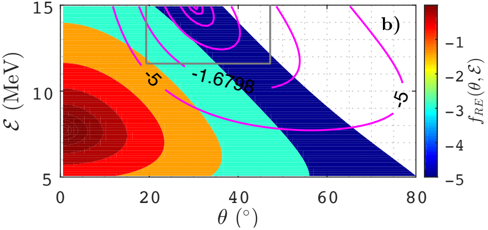

the initial energy and pitch-angle distribution is given by

$$\mathcal{F}_{RE}(\theta, \mathcal{E}, t = 0) = \frac{f_{RE}(\theta, \mathcal{E}) \times P_R(\theta, \mathcal{E}, \lambda, B_0)}{P_T}$$

where f_{RE} is the RE distribution model, P_R is the radiation per particle and P_T is the total radiation.

- Here $f_{RE}(\theta, \mathcal{E}) = f_{\mathcal{E}}(\mathcal{E}) f_\theta(\theta, \mathcal{E})$ where $f_{\mathcal{E}}(\mathcal{E})$ is obtained from the experiment and $f_\theta(\theta, \mathcal{E})$ is the Fokker-Planck model.
- The spatial distribution is taken as uniform.

MODEL VALIDATION USING LARGE-TIME SIMULATIONS

Departures from Fokker-Planck equilibrium distribution

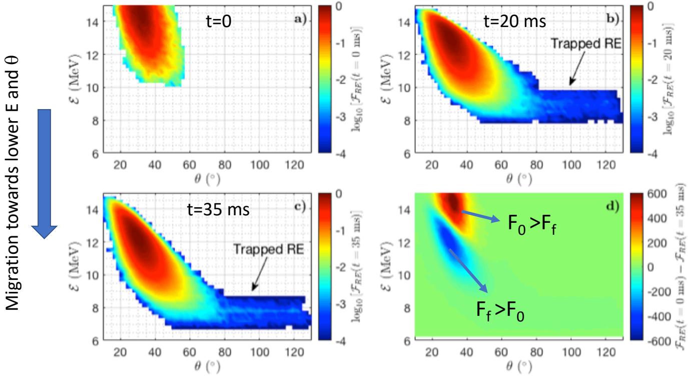

The departure of $\mathcal{F}_{RE}(\theta, \mathcal{E}, t)$ from the initial condition indicates that $f_{RE}(\theta, \mathcal{E}) = f_{\mathcal{E}}(\mathcal{E}) f_{\theta}(\theta, \mathcal{E})$, with $\hat{A} = 1$is not a solution consistent with the full-orbit dynamics in this DIII-D plasma.

Low energy RE do not seem to depart significantly from the Fokker-Planck model. However, higher energy RE rapidly depart from the Fokker-Planck model $\hat{A} = 1$, and converge to $\hat{A} \approx 5$.

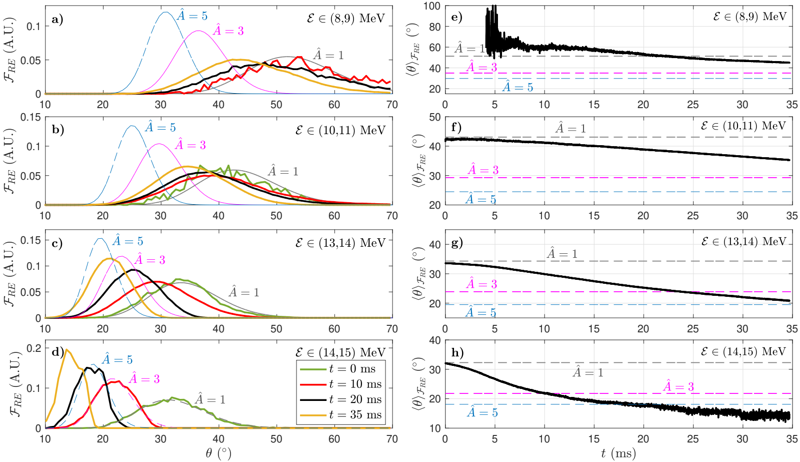

This is in agreement with KORC synchrotron synthetic diagnostic and DIII-D measurenmts.

SPATIO-TEMPORAL DYNAMICS OF MEAN ENERGY AND MEAN PITCH ANGLE

Mean values decrease and mean pitch angle peaks at the edge

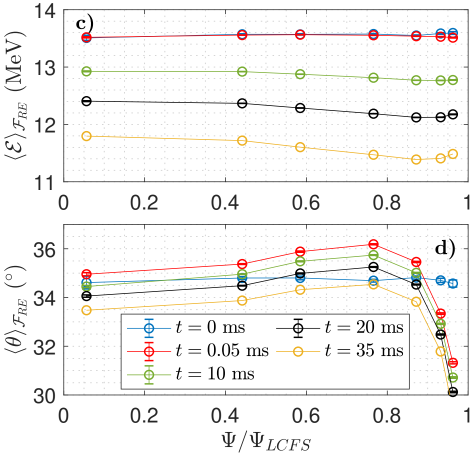

Statistics done of the the RE contributing to the observed synchrotron radiation.

ENERGY DEPENDENCE OF RE DENSITY AND MEAN PITCH ANGLE SPATIAL PROFILES

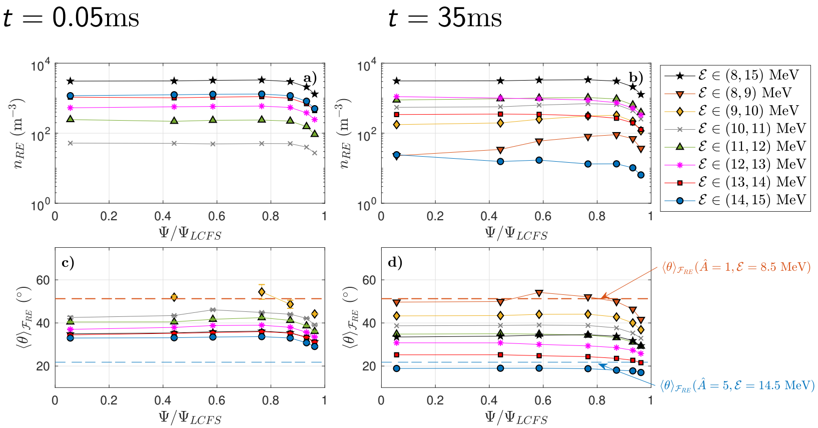

High energy RE rapidly depart from the Fokker-Planck model $\hat{A} = 1$, and converge to $\hat{A} \approx 5$.

CONCLUSIONS

- We have presented a validation study of pitch-angle dynamics models based on 0-D 2-V Fokker-Planck descriptions
- The study was based on two complimentary calculations:
  (i) synchrotron radiation spatial pattern
  (ii) computation (large time) of RE orbits
- It was shown that KORC is able to quantitatively reproduce the synchrotron radiation pattern observed in DIII-D quiescent plasmas.
- In agreement with the experiments it is observed that the Fokker-Planck model does not reproduce the observed and computed decay of the pitch angle distribution ($\hat{A} \neq 1$).
- Long time-dependent KORC simulations show that the 0-D 2-V Fokker-Planck equilibrium distribution is not an equilibrium distribution when spatial orbit effects are taken into consideration